# Route to chaos by irregular periods: Simulations of parallel pumping in ferromagnets

F. Waldner and D. R. Barberis
*Physics Institute, University of Zurich, CH-8001 Zurich, Switzerland*

H. Yamazaki
*Department of Physics, Faculty of Science, Okayama University, Tsushima, Okayama 700, Japan*
(Received 20 August 1984)

A peculiar route to chaos is known experimentally for magnetic parallel pumping. The periods of auto-oscillations become irregular at the onset of chaos, without previous cascades of period-doubling bifurcations. This route to chaos has been found by the simulation of parallel pumping of a single spin interacting with a cavity or, for multispin systems, coupled by exchange.

## I. INTRODUCTION

Nonlinear systems which undergo transitions from stationary to periodic and chaotic states are usually classified according to their route to chaos. The route to chaos by a cascade of period-doubling bifurcations is well established.[1]

Here, a different route by "irregular periods" will be considered. It might be present in many systems showing auto-oscillations, if these oscillations are allowed to vary their frequency continuously. It could also be found in systems having a cascade of period-doubling bifurcations, if the parameters are set accordingly. In Fourier spectra, irregular periods will broaden the Fourier peaks, while period doubling will create additional peaks at fractional frequencies. A combination of both routes would create a chaotic regime before the full cascade of period-doubling bifurcations is developed.

Magnetic resonances in ferro- and antiferromagnets provide examples of both routes. Yamazaki[2] described period doubling under parallel pumping in an antiferromagnet in accord with the theoretical predictions of Nakamura *et al.*[3] Gibson and Jeffries[4] reported a similar behavior for ferromagnetic resonant in yttrium iron garnet (YIG). In addition, they write "Another, quite different, signal shape is shown . . . reminiscent of relaxation oscillations in general; in fact, Hartwick *et al.*[5] in their discovery of auto-oscillations described them as relaxation oscillations. We believe that these are distinct phenomena but have not investigated their possibly chaotic dynamics." Indeed, Fig. 6(a) in Ref. 4 shows a scatter in the time intervals between consecutive spikes, i.e., it is chaotic with irregular periods. Recently, even more pronounced irregular periods of relaxation oscillations were found in parallel pumping experiments, performed in ferro- and antiferromagnets with low threshold powers. Typical examples are shown in Fig. 1, and the experiments are described elsewhere.[6]

Unfortunately, earlier reports on auto-oscillations[5,7,8] in magnetic resonance do not, to our knowledge, display records of these oscillations. Therefore, they cannot be tested for irregular periods.

Using the method introduced by Zakharov *et al.*[9] for the description of parallel pumping, Grankin *et al.*[10] and Nakamura *et al.*[3] have simulated the chaotic regime for two interacting spin-wave pairs. One paper[3] reports numerical results showing period doubling, the other paper[10] displays Fourier spectra which seem to imply irregular periods without period doubling. Recently, Lugiato *et al.*[11] found irregular periods as numerical solutions of their nonlinear equations for a laser driven by an external field. For different parameter settings, however, the same system exhibits a cascade of period-doubling bifurcations.

It is the aim of this paper to describe a simple model which, first, shows relaxation oscillations, and, second, explores the onset of chaotic behavior by irregular periods. This work is restricted to the simulation of parallel pumping in ferromagnets. After a brief introduction to parallel pumping, models are presented which describe the experimental situation closely. First the Landau-Lifshitz equations are used to describe the motion of a classical spin in a cavity, where the interaction with the cavity is represented by equations for a damped $LC$ circuit. A second model treats a chain of exchange coupled spins, also driven by a parallel pumping field. Numerical simulations are presented which illustrate relaxation oscillations and steps on the route to chaos by irregular periods.

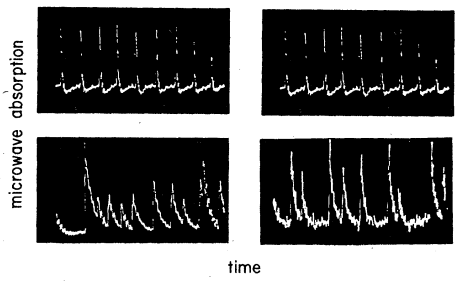


FIG. 1. Relaxation oscillations measured by parallel pumping, showing nearly regular and irregular periods in the 10-kHz region, in the antiferromagnet $(NH_3)_2(CH_2)_2CuCl_4$ at 9.36 GHz, 0.88 T, 1.4 K.

 

## II. MODELS FOR PARALLEL PUMPING

### A. Introduction to parallel pumping (Ref. 12)

For the usual magnetic resonance one applies an oscillating field *normal* to the static field $\vec{H}_0$. For parallel pumping, however, both oscillating and static field are *parallel.* Further, the pumping frequency is about twice the Larmor frequency of the spin system. Why does this field couple to the motion of the spins? The point is that a nonlinear term breaks the axial symmetry along $\vec{H}_0$. This might be done, for example, by a crystalline anisotropy energy $DS_x^2$, while $\vec{H}_0$ is along the $z$ axis. Then, the spins will precess along an elliptical path with their $z$ component oscillating at twice the Larmor frequency $\omega_L$. Therefore, this oscillation can be driven by the external pumping field along the $z$ axis, oscillating at $\omega_p \simeq 2\omega_L$. Usually, this driving is explained in terms of the excitation of spin waves or magnon pairs with small and opposite wave vectors $\vec{k}$. Here, we assume models which describe the motions of the spins classically.

### B. Model for one spin in a cavity

We use the following model for parallel pumping in ferromagnets: A single classical spin is described by an equation of motion with Landau-Lifshitz damping. Due to the inclusion of anisotropic terms, the description is in the laboratory frame. In addition, the microwave cavity is represented by a damped resonant circuit. The corresponding Kirchhoff equations include radiation damping effects along the $z$ axis. In order to facilitate computations, these "Landau-Lifshitz-Kirchhoff" (LLK) equations are given in normalized parameters.

The equation of motion has the form[12]

$$\frac{d\vec{s}}{dt} = \vec{s} \times \vec{h} - \lambda \vec{s} \times (\vec{s} \times \vec{h}) \tag{1}$$

for a classical spin vector $\vec{s}$ of unit length $|\vec{s}| = 1$ in an effective normalized field $\vec{h} = \gamma \vec{H}$ (gyromagnetic ratio $\gamma$, effective magnetic field $\vec{H}$), where $\lambda$ is the Landau-Lifshitz damping parameter. The effective field $\vec{h}$

$$\vec{h} = (h_0 + \alpha h_p + a)\vec{e}_z - h_A \vec{e}_x \tag{1a}$$

is the sum of the static field $h_0$, the pumping field $h_p = h_{p0} \sin(\omega_p t)$, and the field $a(t)$ of the cavity along the $z$ axis with unit vector $\vec{e}_z$, and an anisotropy field $h_A = d_A s_x$ along the $x$ axis, representing an anisotropy energy term with a hard $x$ axis and an easy $yz$ plane. (The factor $\alpha$ will be described later.) The Larmor precession frequency $\omega_L$ for small polar angles $\theta$ of the spin is[12]

$$\omega_L = [h_0(h_0 + h_A)]^{1/2} \tag{1b}$$

and $\omega_L$ decreases with increasing angle $\theta$ due to the nonlinear anisotropy term.

For parallel pumping, the sample is at a position inside the microwave cavity where the pumping field is parallel to the static field $\vec{H}_0$. The sample is affected also by the radiation field, whose $z$ component is enhanced by the cavity. For steady-state conditions, this interaction acts as an additional damping ("radiation damping"). If the spin opens its precession cone, the cavity will create a larger damping field with some time delay. Usually, this retarding effect is neglected. For highly nonlinear systems, however, such small effects might change the time evolution drastically. Therefore, the cavity will be represented by a damped $LC$ circuit. In normalized parameters, the following Kirchhoff equations describe this $LC$ circuit:

$$\frac{da}{dt} = -\gamma_1 a - \omega_c^2 b - B_p \frac{dh_p}{dt} - B_s \frac{ds_z}{dt} , \tag{2a}$$

$$\frac{db}{dt} = -\gamma_2 b + a . \tag{2b}$$

The parameter $a(t)$ is the normalized field produced by the coil at the position of the sample and is proportional to the current in the coil. The parameter $b(t)$ is proportional to the charge on the capacitor, $\gamma_1$ and $\gamma_2$ describe series and parallel damping, respectively, and $\omega_c$ is the resonance frequency of the undamped circuit. The values $B_p$ and $B_s$ contain the coupling for the induction in the coil by the pumping field $h_p(t)$ and by the precessing magnetic moment, which is in turn proportional to $s_z(t)$. [Since Eqs. (2a) and (2b) are linear, the external pumping field could also be added directly by setting $\alpha = 1$ and $B_p = 0$.] Further, dimensionless parameters can be obtained by introducing a normalized time $t' = t/2T_p$, with $2T_p$ being the period of the forced spin precession for steady-state pumping.

### C. Comparison with the Maxwell-Bloch and Bloch-Kirchhoff models

It is interesting to compare the above LLK equations with the Maxwell-Bloch (MB) equations used by Lugiato *et al.*[11] to describe an optical laser driven by an external pumping field and with the Bloch-Kirchhoff (BK) equations proposed by Brun *et al.*[13] for their nuclear magnetic resonance laser. Both models are equivalent. The atomic or nuclear spin system is described by one complex parameter (atomic polarization or spin component normal to the precession axis, respectively) and one real parameter (population difference or spin component along the rotation axis) in a frame rotating with the pumping field. In both cases the resonator (mirrors or $LC$ circuit) is represented by one complex parameter only, since the Kirchhoff equations are truncated to one differential equation of first order. This approximation treats only motions which are slow relative to the Larmor precession.

In contrast, the LLK equations are written in a fixed laboratory frame, because the crystalline anisotropy term prevents a transformation to a rotating frame. Therefore, the full time evolution has to be calculated including the Larmor precession itself. The motion of the spin of constant length is described by polar and azimuthal angles which correspond to one complex parameter. In addition, the untruncated equations for the resonator have two variables, both with an amplitude and a relative phase, corresponding to two complex parameters. Therefore, the full

parameter space is larger, although it is easier to describe the spin system itself, since time trajectories for LLK are two dimensional on the surface of the unit sphere, while they are three dimensional (inside a sphere) for MB and BK.

### D. Model for a multispin system

Parallel pumping can be described as the creation of standing spin waves at about half the pumping frequency, or, as the creation of magnon pairs with small and opposite wave vectors $\vec{k}$. Due to the nonlinearity of the problem, these spin waves or magnons interact with further spin waves or magnons. In an elegant analysis, Nakamura *et al.*[3] found the route to chaos by period-doubling bifurcations for pumped spin waves which interact with one additional standing spin wave. To describe this coupling, he included a four magnon interaction (two interacting magnon pairs).

In order to study higher-order interactions with several additional spin-wave pairs, a simple classical approach will be used here. A chain of $N$ discrete spins $\vec{s}_i$ are coupled by nearest-neighbor isotropic Heisenberg exchange interactions. The time evolution of this multispin system is described by a set of $N$ equations (1), each with an additional term $\vec{h}_{ex,i}$ for the effective field $\vec{h}$

$$\vec{h}_{ex,i}=A(\vec{s}_{i-1}+\vec{s}_{i+1}) , \tag{3}$$

where $A$ denotes the normalized exchange constant. The same method has been used to calculate the turbulent behavior of domain walls in strong static fields.[14] Parallel pumping of such a multispin system shows chaos by irregular periods without the need for an interacting cavity. Hence Eq. (2) will not be included in these "Landau-Lifshitz-Heisenberg" (LLH) equations (1) and (3).

## III. NUMERICAL RESULTS FOR ONE SPIN IN A CAVITY

The LLK Eqs. (1) and (2) representing one spin in a cavity were solved numerically by calculating time evolutions ("runs") on a computer. After a few remarks about the numerical procedure, a typical example for irregular periods will be presented by displaying different aspects of the same run. Then, several runs will illustrate the gradual development of periodic relaxation oscillations, including also a merging of two attractors. Finally, the onset of chaotic behavior will be shown followed by a few runs exhibiting a rather stochastic regime.

### A. Remarks about the numerical procedure

The trajectories of the precessing spin were calculated in small time steps (typical 1400—2800 steps for one Larmor period). A variation of these steps did not change the solutions, except for very chaotic regimes, where the deviations grew slowly and approximately logarithmically, as expected for strange attractors.

Although the trajectories of the spins were calculated along the entire path in the laboratory frame, only snapshots at times $t=n2T_p$, i.e., $t'=n$, will be displayed. Thus, a steady-state pumping would give constant values. Further, functions averaged over $2T_p$ will be evaluated and plotted, yielding results which could be compared with measurable quantities. Parameter values and initial conditions were chosen rather to restrict computing time than to quantitatively simulate the experiments.

### B. An illustrative example for irregular periods

In this section, a typical example for irregular periods will be displayed. Different aspects of the same run will be presented. This run has a pronounced scatter in the periods between spikes of comparable amplitudes. Figure 2(a) gives a periodically strobed view of the polar angle $\theta(n)$ of the spin versus the normalized time $t'=n$.

Figure 2(b) shows a function $f(n)$ which is proportional to the power absorbed by the spin system. This function can be compared to the absorption signals of parallel pumping experiments, and it is proportional to $s_z\cos(\omega_p t)$, averaged over $2T_p$ and plotted at normalized times $t'=n$.

Again averaged over $2T_p$, Fig. 2(c) shows the parameter $b(n)$ as a measure of the voltage across the resonating capacitor. Clearly, the periods are unequal. Longer runs

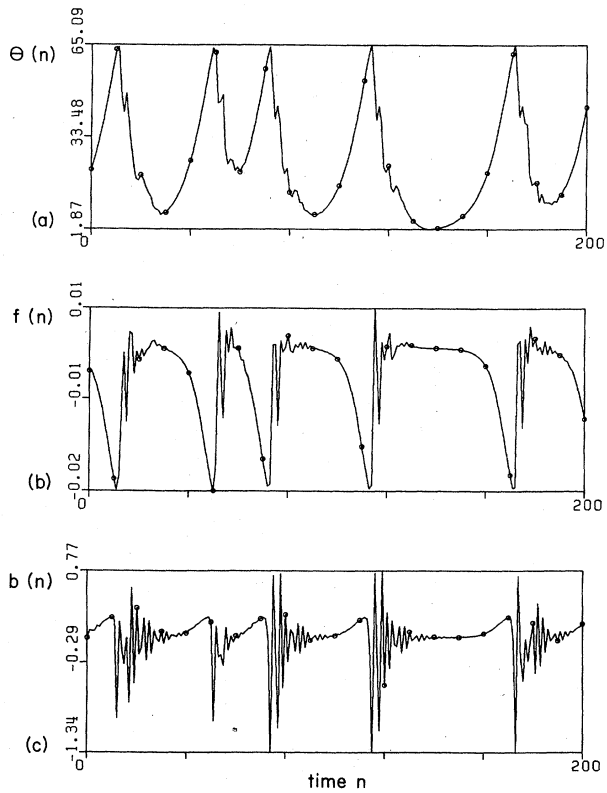


FIG. 2. Numerical simulation for parallel pumping of one spin in a cavity. (a) Polar angle $\theta(n)$ vs normalized time $t'=n$. (b) Function $f(n)$, see text. (c) $b(n)$ of Eq. (2b). To ease the counting of the time $t'=n$, each tenth data point is marked by a circle. [The parameter values for the LLK Eqs. (1) and (2) are: $\lambda=0.01$, $h_0/2\pi=0.85$, $h_{p0}=0.600$, $d_A/2\pi=0.3$, $\omega_p/2\pi=2$, $\gamma_1=3.6\times10^{-3}$, $\gamma_2=0.36$, $\omega_c/2\pi=0.57$, $B_p=8\times10^{-4}$, $B_s=4500$; with initial conditions $\theta_0=20°$, $\phi_0=-70°$.]

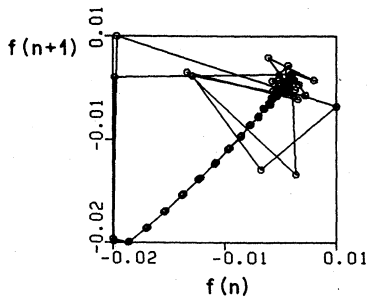


FIG. 3. Return map for $f(n)$ for the strobed times $n=100$–$200$. In contrast to Fig. 2, each data point is marked by a circle. Consecutive points are connected by straight lines.

(displayed later) confirm that their scatter is irregular.

A further interesting feature is best seen in Fig. 2(c). Each spike triggers a damped oscillation with a period $T$ of twice the strobe period, i.e., with $T=2(2T_p)$. However, a closer look indicates that this pattern could be due to a beating with a damped oscillation of a slightly different period. (To ease the counting of the beats each tenth data point is marked by a circle.) Keeping in mind that the anisotropy energy makes the Larmor precession dependent on the polar angle of the spin precession, this pattern could be caused by triggering the free-running precession as a transient feature. Such effects of variable detuning are probably an important ingredient for the creation of irregular periods.

Figure 3 displays a return map $f(n+1)$ versus $f(n)$ for the time $n=100$–$200$. Here, each data point is marked by a circle, and consecutive points are connected by straight lines in order to illustrate the time sequence. The points follow about the same path for the leading edges of each spike, whereas the trailing edges give a rather stochastic pattern.

Figure 4, however, demonstrates that the path of the spins is different for consecutive spikes. In Fig. 4, the trajectories of the spin are plotted, strobed at times $t'=n$, for the time interval $n=100$–$200$. Again, each data point is marked by a circle and consecutive points are connected by straight lines. Since the spin moves on the surface of the unit sphere, Fig. 4(a) gives a "top view" and Fig. 4(b) a "side view" of the sphere, i.e., the projection of the trajectories onto the $(s_x,s_y)$ and the $(s_x,s_z)$ planes are shown. An indication of some kind of twofold rotation symmetry around the $z$ axis in these patterns will be discussed later.

### C. Periodic relaxation oscillations and the merging of two attractors

In this section, the gradual development of periodic relaxation oscillations with increasing pumping power is illustrated. All other parameters of the system, including the initial conditions, were not changed for these runs. Only the function $f(n)$ and top and side views of the trajectories are displayed.

For the run shown in Fig. 5(a), no pumping was applied. Starting at a nonequilibrium condition, the spin relaxes towards the up position parallel to the static field $h_0$. The coupling of the spin precession with the resonator results in a damped oscillatory behavior of $f(n)$ exhibiting an overshoot. It seems plausible that the auto-oscillations of the system observed under conditions of strong pumping are governed by this oscillatory mechanism which is inherent to the system. After the initial transient, the spin is almost exactly along the $z$ axis, as displayed in the top and side views of the strobed trajectories for the time $n=100$–$200$. Obviously, the trajectories are reduced to a single point at the up position (polar angle $\theta=0$), and this point is a stable fixed point.

In the next run shown in Fig. 5(b), a pumping amplitude $h_{p0}\equiv\hbar_{p0}/2\pi=0.300$ drives the system into a steady-state pumping condition above threshold. In this steady state, the spin precesses along the same elliptical path. Thus, the spin has the same direction after each full Larmor precession forced by the pump. Strobing after intervals $2T_p$ gives a single point on the surface of the unit sphere. This point seen in the top and side views of Fig. 5(b) is a stable fixed point while the up position ($\theta=0$) is now an unstable fixed point. A spin with $\theta\neq0$ will reach the stable fixed point through a damped auto-oscillation, as seen for $f(n)$.

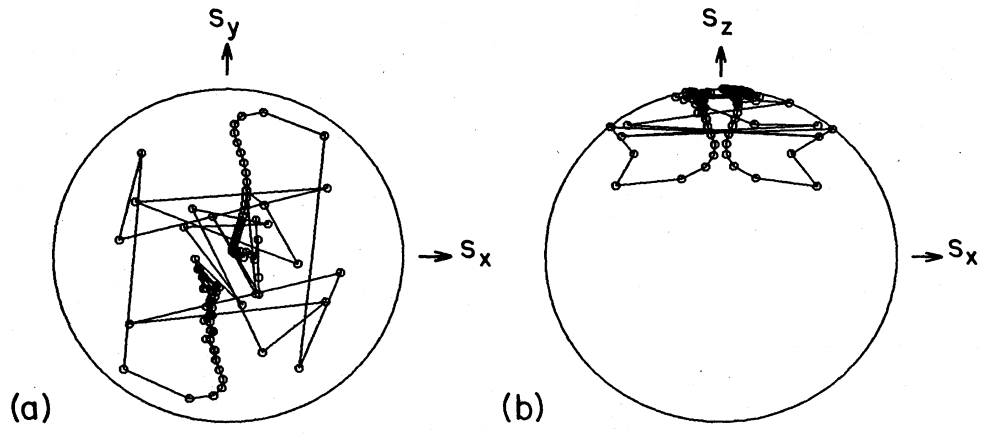


FIG. 4. Trajectories of the spin projected onto: (a) $(s_x,s_y)$ plane, (b) $(s_x,s_z)$ plane. Each data point is marked by a circle, and consecutive points at the strobed times $n=100$–$200$ are connected by straight lines.

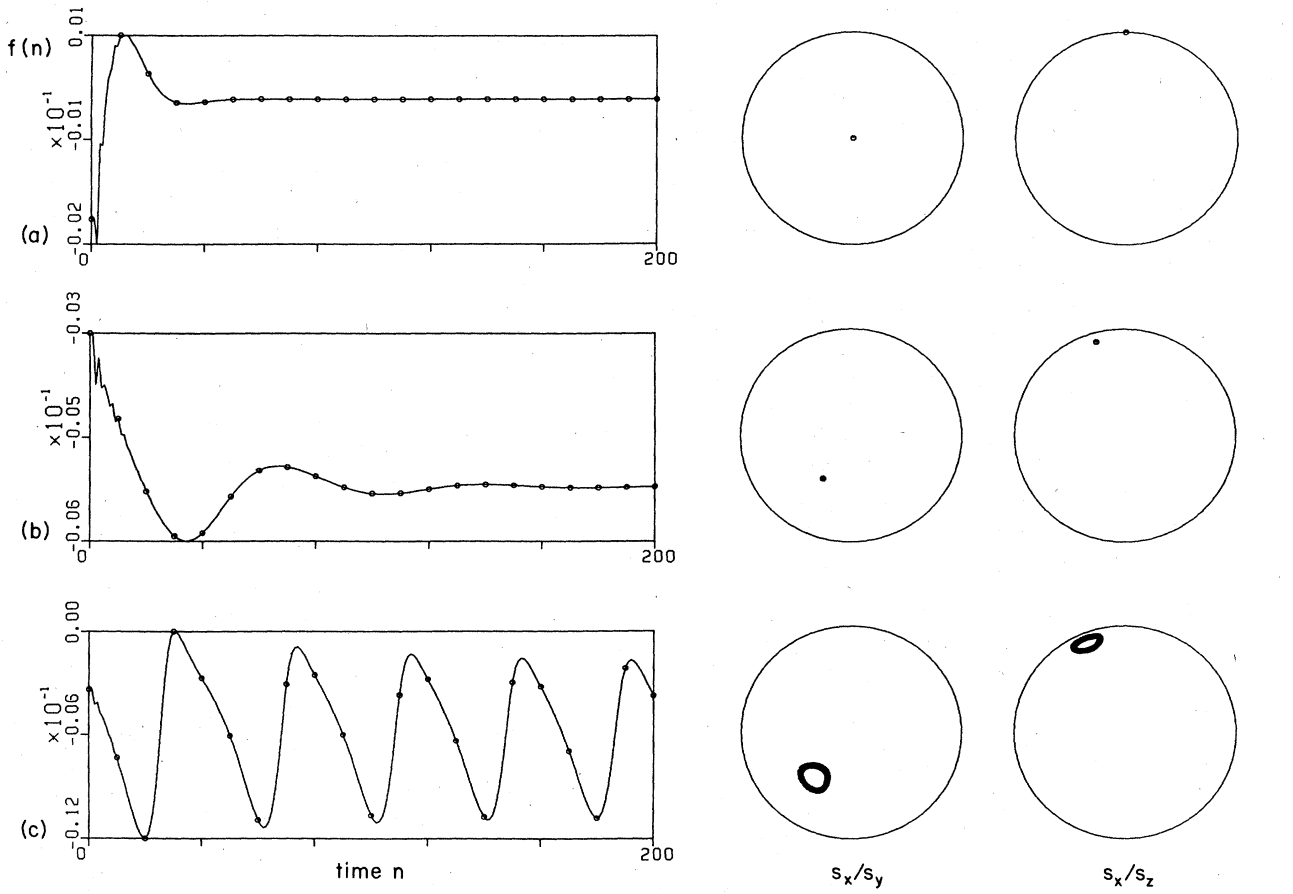


FIG. 5. Numerical simulation for parallel pumping of one spin in a cavity for different values of the pumping amplitude $h_{p0}$. (For all other parameters, see caption of Fig. 2.) Left: $f(n)$ vs time $n=0$—200; circles: every tenth data point. Right: strobed trajectories of the spin projected onto the $(s_x,s_y)$ plane and $(s_x,s_z)$ plane, respectively, for the strobed times $n=100$—200; circles: every data point. The pumping amplitudes $h_{p0}$ are: (a) (top) 0, (b) (center) 0.300, (c) (bottom) 0.360; showing: (a) relaxation to the up position, (b) relaxation to a steady-state pumping, (c) relaxation to a periodic limit cycle.

Due to the peculiar symmetry of parallel pumping, there is a second stable fixed point at the same polar angle, related to the first point by a 180° rotation about the $z$ axis. More precisely, the system has a twofold rotation symmetry about the $z$ axis if the static and dynamic fields $h_0$ and $h_p$ lie exactly in the easy plane of the anisotropy term $DS_x^2$. This rotation symmetry is related to the fact that the pumping field goes through two maxima while the spin precesses around once. Moreover, each of the two stable fixed points, representing a steady-state pumping, will attract only one half of the possible initial conditions, i.e., half of the surface of the unit sphere, excluding the unstable fixed points $\theta=0°,180°$. At a higher pumping field of $h_{p0}=0.360$, the auto-oscillation of the system is not damped away. Figure 5(c) shows an attractor in the form of a limit cycle.

All runs displayed in Fig. 5 show the time evolution starting at the initial condition. Longer runs reveal that after about 200 time steps the system is rather close to the limiting behavior for long times. Since this limiting behavior is the primary interest, the next Figs. 6 and 7 only display the time evolution for the time steps $n=200$—400.

For increasing pumping amplitudes, it is obvious that the trajectory of the limit cycle shown in Fig. 5(c) will enlarge. By doing so, the variation of the polar angle $\theta$ also enlarges. Since the interaction of the spin system with the pumping and the radiation damping field is smaller for smaller angles $\theta$ and is zero for the up position ($\theta=0°$), the speed along the trajectory is increased for large angles and slowed down for small angles $\theta$. This deforms the oscillation into the shape of spikes with intervals of small values of $f(n)$. This qualitative explanation of the shape of the experimental relaxation oscillation is illustrated in Fig. 6 for the pumping amplitudes $h_{p0}=0.400$, 0.410, 0.415, respectively. For all these values, the behavior is periodic, and the function $f(n)$ does not change much, except that the period increases from Fig. 6(a) to Fig. 6(b) and decreases from Fig. 6(b) to Fig. 6(c). This effect can be attributed to the merging of two attractors and will be explained by discussing the trajectories.

Keeping in mind that the problem has an inherent twofold rotation symmetry about the $z$ axis, the limit cycle of Fig. 6(a) has a counterpart which is not reached from the chosen initial condition. The existence of this counterpart is easily seen in Fig. 6(b), where the same initial condition

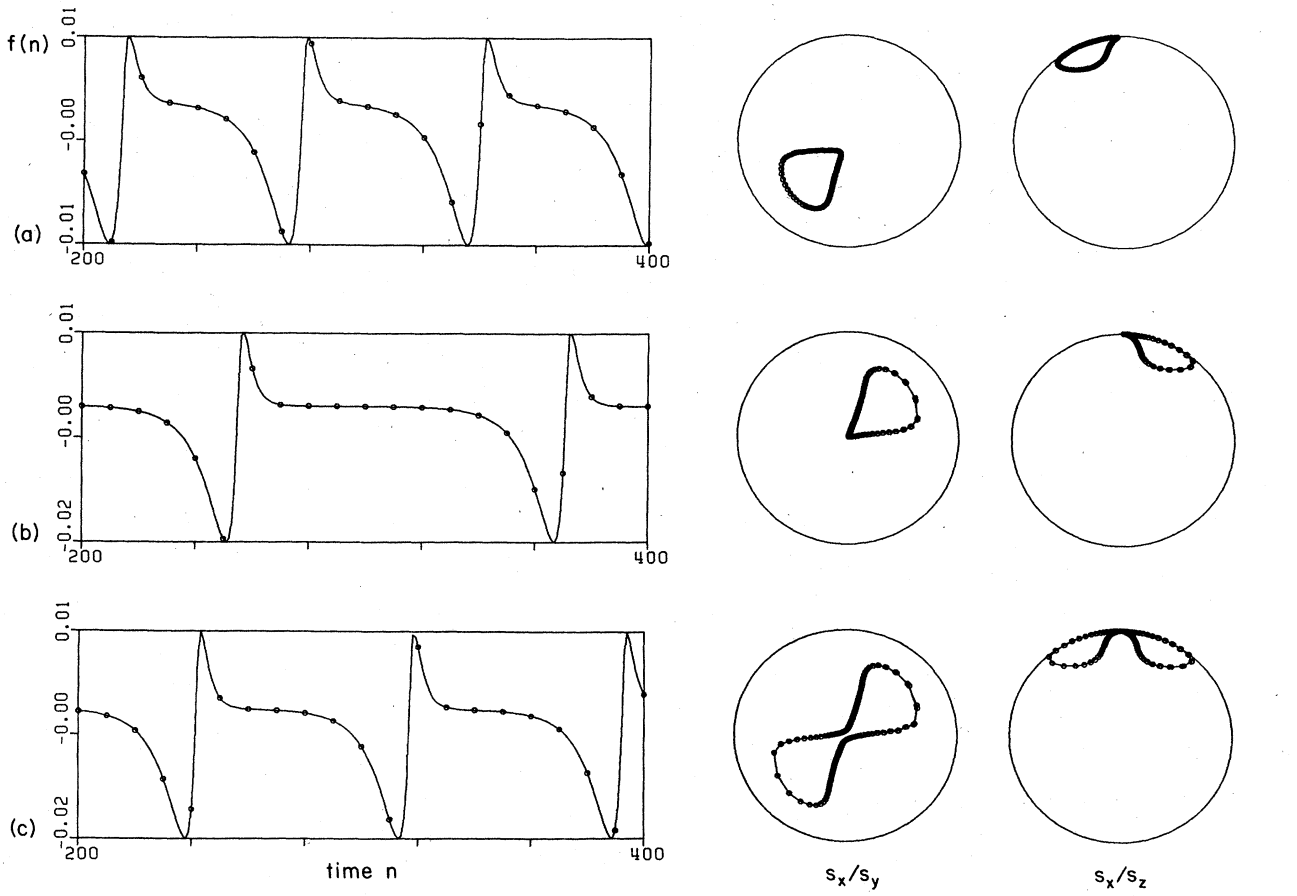


FIG. 6. Same as Fig. 5, except: time $n=200$–400 for $f(n)$ and trajectories; $h_{p0}$: (a) 0.400, (b) 0.410, (c) 0.415; showing the shape of periodic relaxation oscillations with trajectories along: (a) one limit cycle, (b) the other limit cycle, (c) a merged limit cycle.

is connected to the other cycle. It is natural to imagine that for increased pumping amplitudes the enlarged limit cycles (attractors) will come into contact and merge into one limit cycle. Figure 6(c) shows such a coalesced cycle with twofold rotation symmetry. Assuming that the attractors come into contact at one point only, this point must be the up position in order to conserve the twofold rotation symmetry. Since the up position is a fixed point, the period of the relaxation oscillation diverges at the exact merging condition. The simulations reveal that, indeed, the periods increase when the merging condition is approached from below or above. Although the system bifurcates for decreasing power from one to two attractors, combined with a "slowing down" of the motion, this behavior is not a second-order phase transition in the strict sense, since no thermodynamic fluctuations are involved.

### D. The transition from regular to irregular periods and to strongly chaotic behavior

In this section, it will be illustrated that the mismatch between the period forced by the pumping and the Larmor period of the spin results in irregular trajectories. As a consequence, the periods between the spikes become irregular. Finally, the behavior is strongly chaotic for very large pumping fields.

Figure 7(a) displays a regular relaxation oscillation for a pumping amplitude $h_{p0}=0.450$. There is a rapid change of the polar and azimuthal angles during the spiking. This triggers a transient Larmor precession. The resulting beat of the Larmor precession frequency with the pumping frequency is seen as a zigzag in the trajectories strobed with half the pumping frequency. During the time interval between two spikes the transient oscillation is damped away. The next transient is locked to the pumping. The same beat pattern repeats and, therefore, the regime is periodic.

For the run evaluated for $h_{p0}=0.465$ [Fig. 7(b)] the system is in the chaotic regime. Both amplitudes and periods are irregular, although their scatter is small. The scatter of the periods is easily seen by comparing the data points marked by circles (each tenth point) of Figs. 7(a) and 7(b). The reason for the irregular behavior is best seen in the trajectories. The zigzag paths do not repeat. The transient triggered by a spike is not fully damped until the next spike starts. Since the self-oscillation of the system is probably not commensurate with the pumping, the pumping and the phase lag of the self-oscillation are responsible for the triggering of a new spike. Therefore,

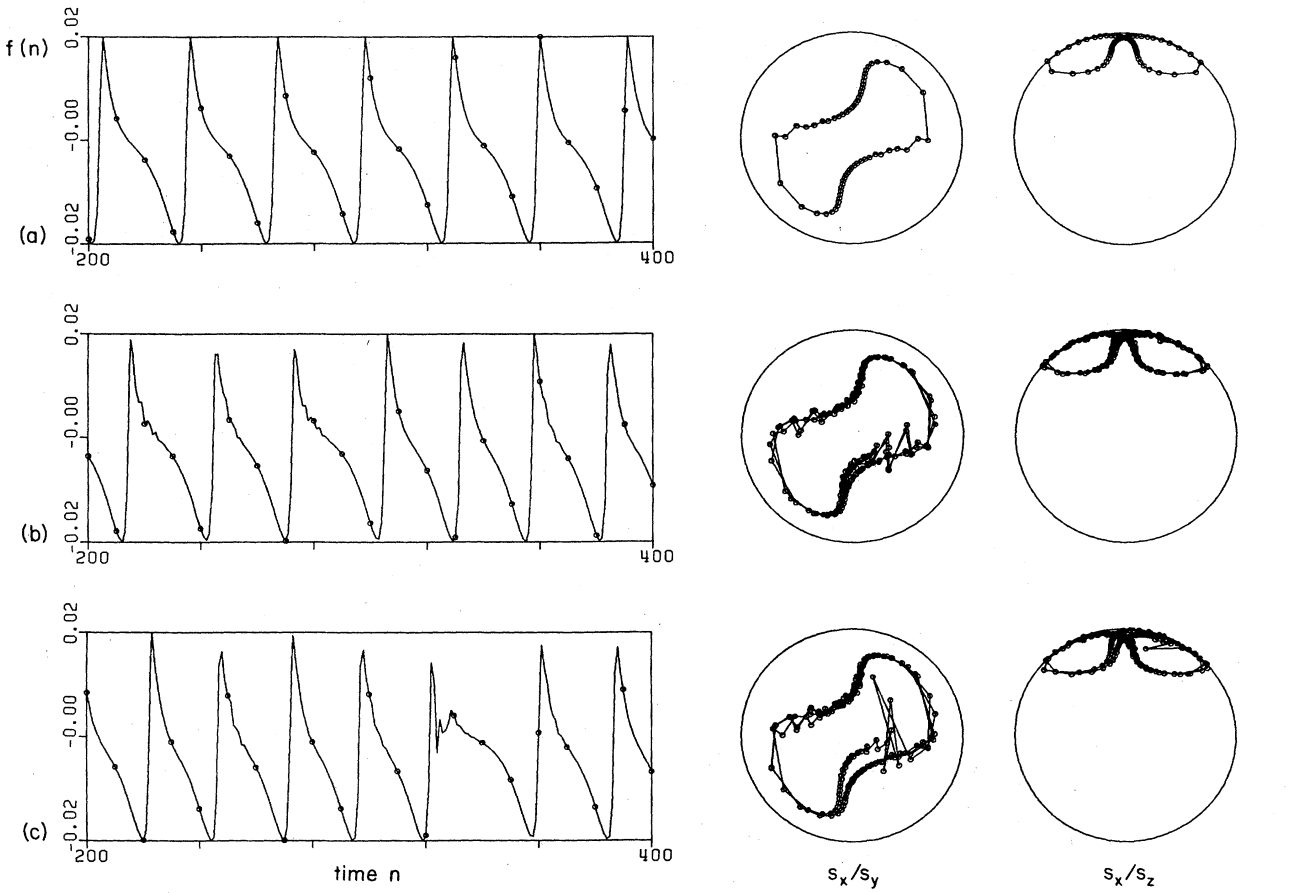


FIG. 7. Same as Fig. 5, except: time $n=200$–400 for $f(n)$ and trajectories; $h_{p0}$: (a) 0.450, (b) 0.465, (c) 0.470; showing: (a) regular periods slightly below, (b) irregular periods slightly above the transition to chaotic behavior, (c) a more pronounced scatter in the periods and amplitudes of $f(n)$ related to more complex trajectories.

this triggering occurs after variable time intervals.

At a slightly higher pumping amplitude $h_{p0}=0.470$ [Fig. 7(c)] the irregularities of the time intervals are stronger. A pronounced zigzag might end at a smaller polar angle for which the speed along the trajectory is slowed down. This creates a much longer interval to the next spike.

For the pumping amplitude $h_{p0}=0.600$, the irregularities have increased, see Fig. 8(a). For the last two runs shown in Figs. 8(b) and 8(c) for $h_{p0}=1.000$ and 4.000, respectively, the system is in the strongly chaotic regime. There is almost no section of smooth behavior, and the resulting function $f(n)$ shows more and more a deterministic broadband noise. The trajectories are typical for strange attractors. The basin of attraction is within a restricted area of the parameter space, here at the upper half of the surface of the unit sphere. Note that the run displayed in Fig. 8(a) is a continuation ($n=200$–400) of the initial time evolution ($n=0$–200) which has been described in Sec. III B (Figs. 2–4).

## IV. NUMERICAL RESULTS FOR A MULTISPIN SYSTEM

### A. Description of the system and the simulations

In this section, we present simulations of a multispin system described by the LLH Eqs. (1) and (3). Here, no cavity is involved, therefore, Eq. (2) is not used. To reduce computing time, only five spins ($N=5$) are arranged in a chain and coupled by isotropic exchange.

The intention is to study the pumping of the uniform mode and the excitation of several nonuniform modes (spin waves). Therefore, the end spins are not pinned, to allow the uniform precession of all spins. The frequencies $\omega_{\mathrm{NM}}$ of the nonuniform modes (NM) are set to the same order of magnitude as the pumping frequency $\omega_p$ ($\omega_{\mathrm{NM}}/\omega_p \simeq 2.0$, 1.7, 1.0, 0.28 for zero static fields). The initial condition was chosen such that all normal modes were excited. Moreover, the pumping amplitudes varied from spin to spin, thus simulating an inhomogeneous pumping field, in order to couple the pumping to all normal modes.

### B. Comparison of two chaotic runs

An important feature of chaotic time evolutions is their extreme sensitivity to small parameter changes. This effect is illustrated by displaying two runs for which the pumping amplitudes have a relative difference of $1.4\times10^{-4}$. In addition, these two runs for a multispin system exhibit patterns of higher complexity than the runs of the previous section for a single spin in a cavity, a fact which is easily understood by a comparison of their parameter spaces: three complex variables of the single-

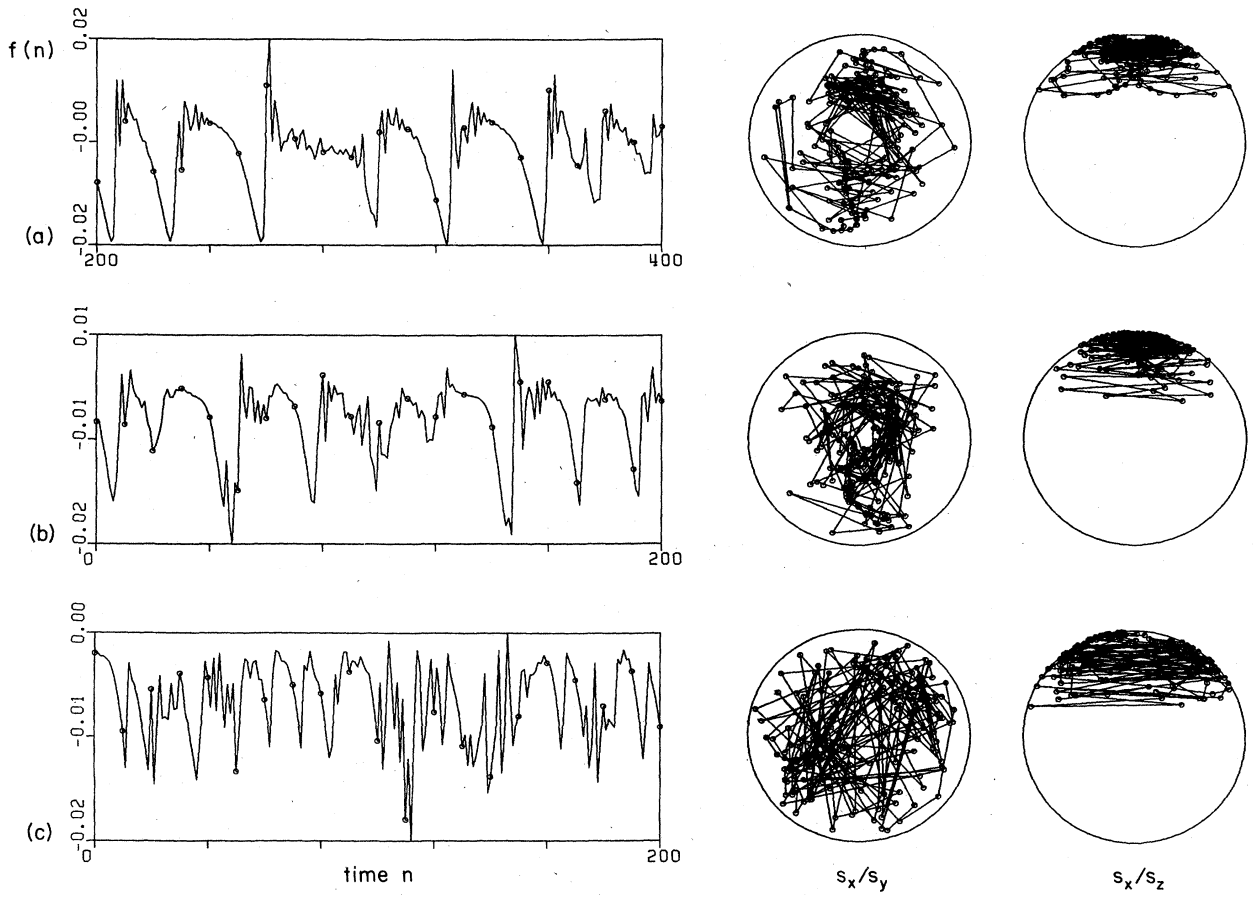


FIG. 8. Same as Fig. 5, except: time $n$ for $f(n)$ and trajectories: (a) 200—400; (b), (c) 0—200; $h_{p0}$: (a) 0.600, (b) 1.000, (c) 4.000; showing: (a) very irregular periods and amplitudes; (b), (c) strongly chaotic behavior resembling broadband noise.

spin systems in a cavity versus five complex variables of the multispin system (five spins, no cavity).

Figures 9 and 10 give strobed plots of the polar angles $\theta_i(n)$ and the azimuthal angles $\phi_i(n)$ of the spins $i=1-5$, and the sum function $f(n)=\sum_i f_i(n)$ for the runs 1 and 2, respectively. Clearly, the spin waves are not damped away. Further, there is a gradual increase of the difference between the two runs for increased normalized time $n$, resulting in very different patterns for larger values of $n$. The functions $f(n)$ seem to correspond to the strongly chaotic regimes of the single-spin system, described in the previous section.

For a better comparison to the single-spin system, the normalized sum vector $\vec{s}=(1/N)\sum_i \vec{s}_i$ was evaluated and its polar and azimuthal angles $\theta,\phi$ plotted in Figs. 11 and 12, together with the strobed trajectories of $\vec{s}$ projected onto the $xy$ and $xz$ planes. (These trajectories are inside the unit sphere since the magnitude of the normalized sum spin $|\vec{s}|$ is smaller than unity when spin waves are excited.)

It is interesting that the trajectories of the sum spin have a qualitatively different pattern than the trajectories of the single-spin system in the strongly chaotic regime as shown in Fig. 8. The sum spin stays in one of the two regions related by twofold rotation symmetry for a number of cycles, and turns over eventually to the other region, where it cycles again but with a different period. It might even come almost to rest for a while during the change-over, when it comes close to the fixed point (up position). The occurrence of such an "intermittency" is very sensitive to the parameters. It is absent for run 2 during the displayed evolution time.

Usually, excitations of coupled systems are analyzed by the determination of the content of normal modes. In the present spin system, there are four nonuniform normal modes (standing spin waves) which are described by their amplitudes and relative phases. However, such a treatment implies a linearization since the superposition principle is not valid for nonlinear problems. This linearization is not practical for large excitations. Indeed, large spin-wave excitations are present as illustrated in Fig. 13. The strobed trajectories of the sum spin (describing the uniform mode) [Fig. 13(a)] might be compared to the strobed trajectories of the spins $i=2$ [Fig. 13(b)] and the end spin $i=5$ [Fig. 13(c)] for the normalized time $n=50-100$ of run 2.

Lacking a convenient numerical method for the decomposition of these excitations into normal modes, a rather crude display is used to illustrate the temporal and spatial structures of the nonuniform spin-wave excitations alone.

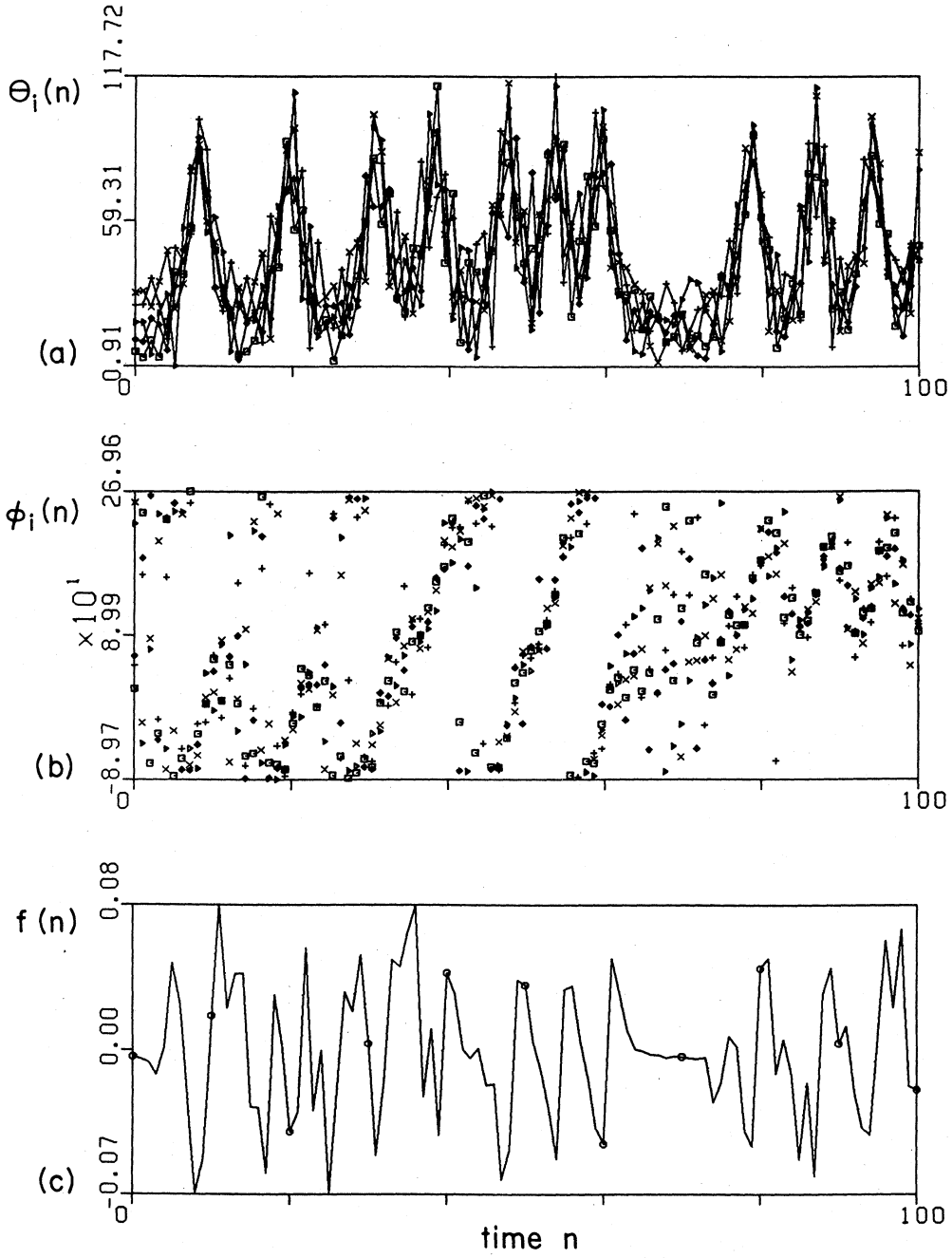


FIG. 9. Numerical simulation for parallel pumping of a multispin system of $N=5$ spins coupled by isotropic Heisenberg exchange. The polar angles $\theta_i(n)$ and the azimuthal angle $\phi_i(n)$ are displayed at the strobed times $n$ in (a) and (b), respectively, with the symbols □, △, ×, +, ◇, for the spins $i=1-5$. (c) Sum function $f(n)$, see text. [The parameter values of the LLH Eqs. (1) and (3) are: $\lambda=0.003$; $h_0=0.8$, $\omega_p/2\pi=2$; $h_{p0,i}=h_{p00}c_i$ with $h_{p00}=0.7$, $c_i=0.98$, 1.00, 0.98, 0.92, 0.82; $d_A/2\pi=0.7$, $A/2\pi=2$. The initial conditions are: $\theta_{i,0}=10.6°$, 21.8°, 26.5°, 22.9°, 13.5°; $\phi_{1,0}=136°$, −25.8°, 127°, −63°, 113°.]

The excess exchange energy proportional to $1-\vec{s}_i\cdot\vec{s}_j$ for the spin pair $\vec{s}_i,\vec{s}_j$ is a measure of nonuniform excitation. Figure 14 displays for each of the five spins (horizontal axis) the sum of this energy of interaction (vertical axis) with its nearest neighbors as a function of time (from back to front). Figure 14 indicates that the spatial structure is chaotic also. Probably, several nonuniform modes are excited and are interacting nonlinearily, influencing the temporal behavior of each spin.

An interplay of spatial and temporal behavior has also

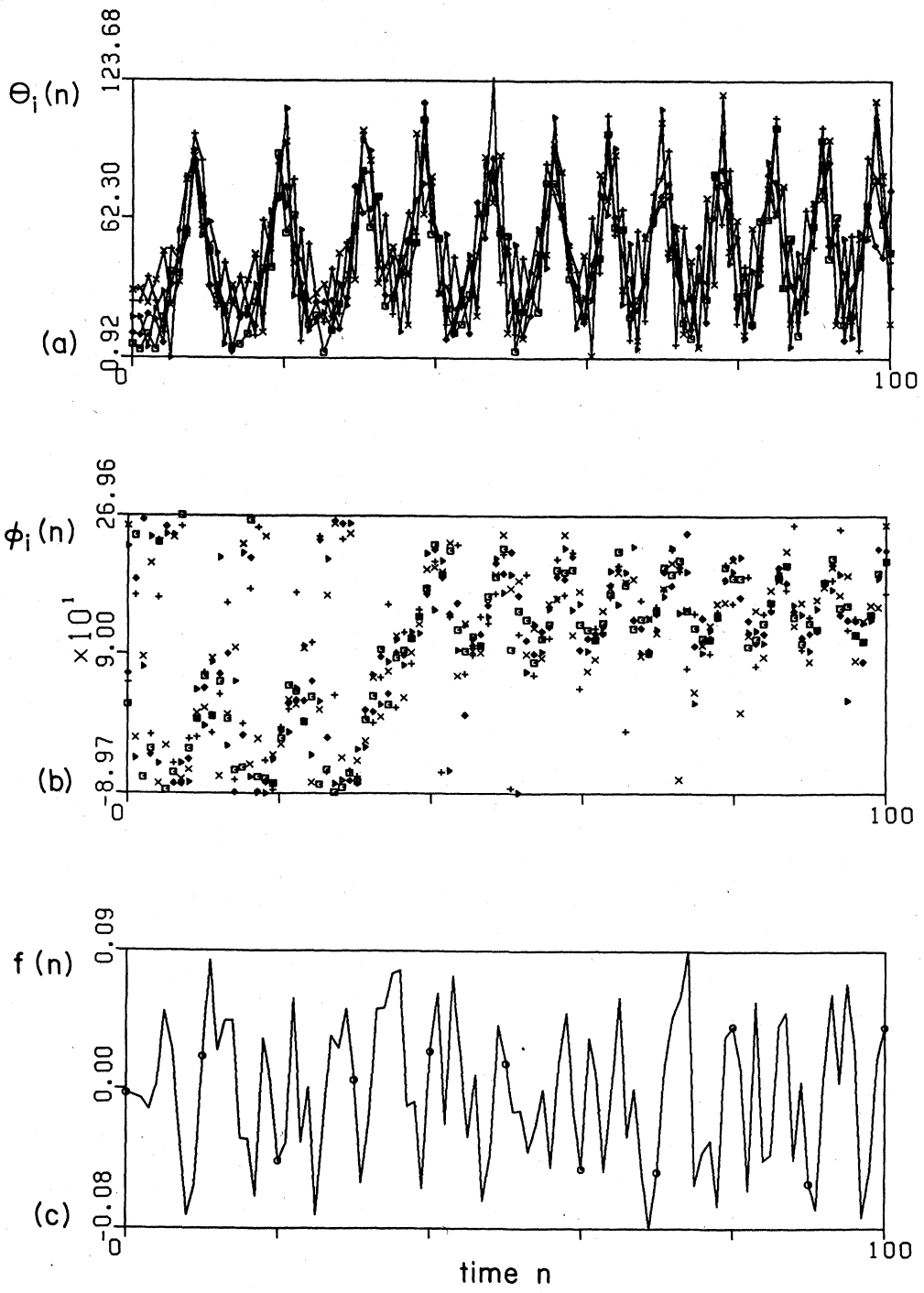


FIG. 10. Same as Fig. 9, except that the pumping amplitude $h_{p00}$ is changed from 0.7000 (Fig. 9: "run 1") to 0.7001 (Fig. 10: "run 2"). Note that the section of nearly smooth behavior observed in run 1 is lacking.

been reported by Bishop *et al.*[15] for a sine-Gordon system exhibiting a route to chaos by period doubling. In contrast to the multispin system (five complex variables), their continuous sine-Gordon system has, in principle, an infinite number of variables.

Experimentally,[6] a rather "broadband noisy" chaotic behavior similar to the simulations for the multispin system has been observed for pumping conditions under which spin waves are excited, with frequencies comparable to the Larmor frequency.

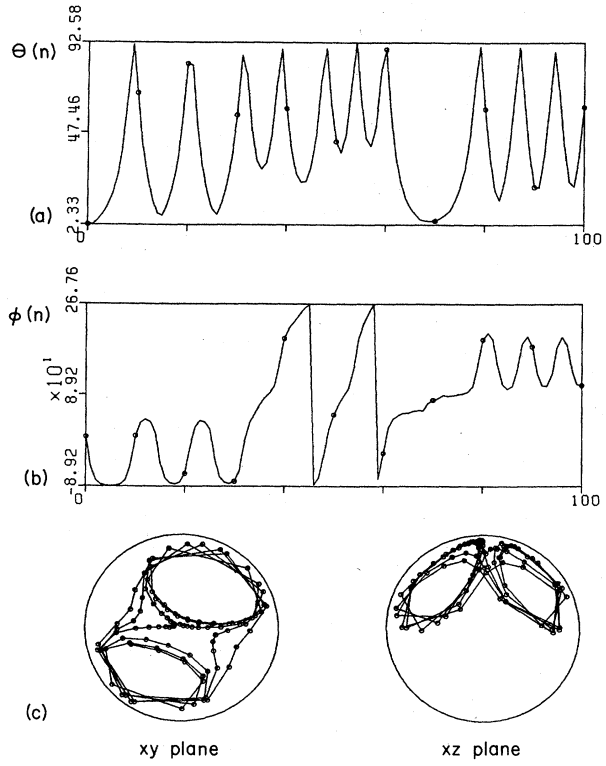


FIG. 11. Run 1, $h_{p00}=0.7000$, normalized sum spin: (a) polar angle $\theta(n)$, (b) azimuthal angle $\phi(n)$ vs time $n$; (c) trajectories of the normalized sum spin $\vec{s}$ projected onto the $xy$ plane and the $xz$ plane at the strobed times $n$.

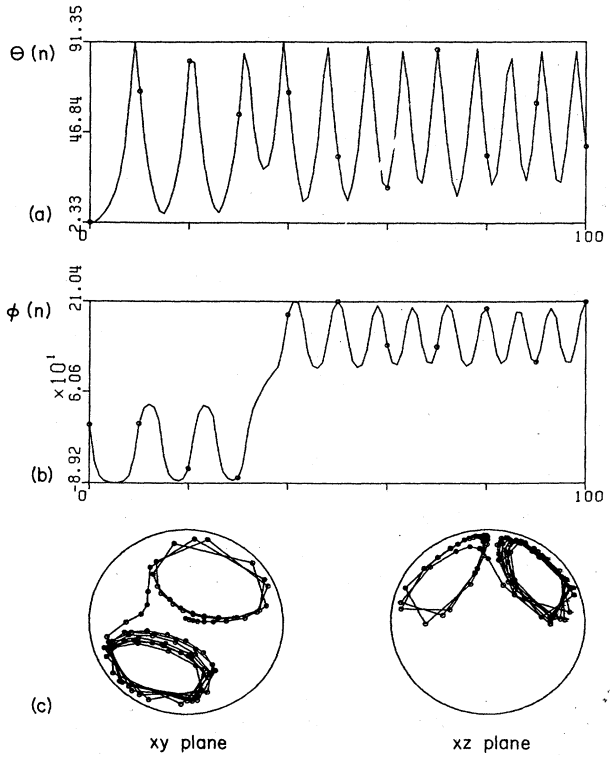


FIG. 12. Run 2, $h_{p00}=0.7001$. Same plots as Fig. 11.

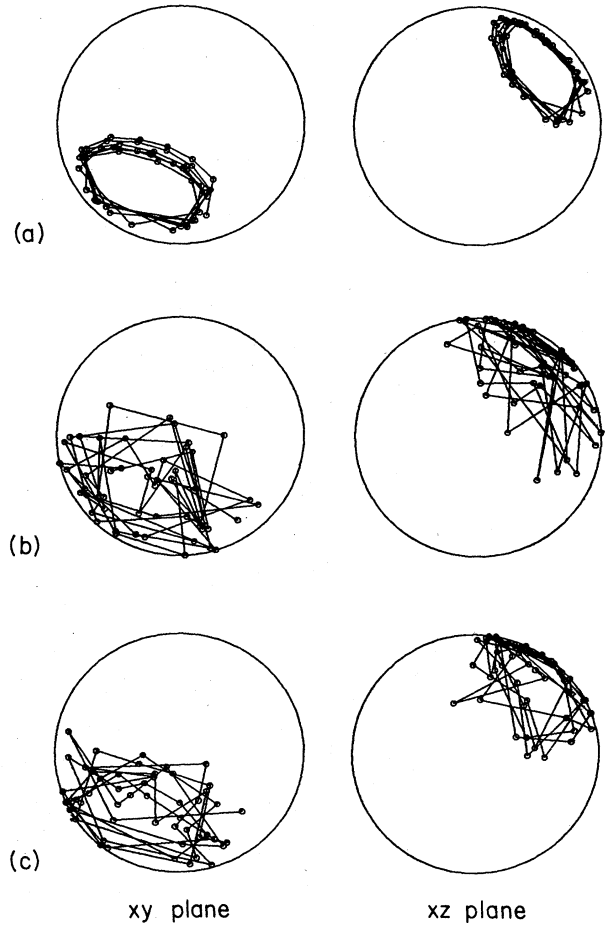


FIG. 13. Run 2, $h_{p00}=0.7001$. Strobed trajectories for the time $n=50-100$ projected onto the $xy$ plane and $xz$ plane. (a) normalized sum spin $\vec{s}$, (b) spin $\vec{s}_i$ $i=3$, (c) end spin $i=5$. The very different patterns indicate strong excitations of nonuniform modes (spin waves).

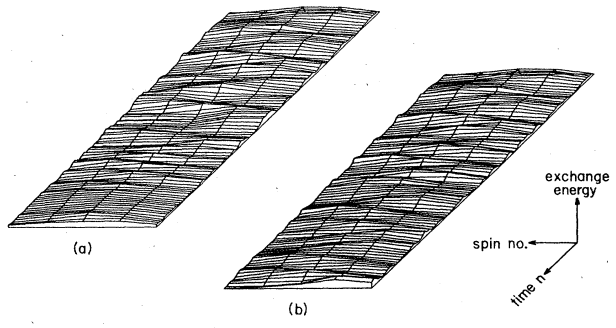


FIG. 14. Spatial and temporal behavior of the exchange energy per spin $\vec{s}_i$ for runs 1 and 2 with $h_{p00}=0.7000$, 0.7001. Horizontal: position of the spin $\vec{s}_i$ in the chain (5 spins); vertical: exchange energy per spin; from back to front: strobed time $n$. Clearly, several normal modes (spin waves) are excited in a chaotic fashion.

## V. CONCLUDING REMARKS

The LLK and LLH equations are used as simple classical models for magnetic parallel pumping. Evidently, only a small portion of the rich variety of solutions have yet been found by numerical simulations. However, their similarity to experimental observations is promising. They describe a peculiar route to chaos by irregular periods without previous cascades of period-doubling bifurcations. It is essential that the processing spin is coupled to one (or more) resonating system(s) such as a cavity or standing spin waves. Further, driving the system slightly off resonance seems to be necessary for the creation of beat patterns between the free and enforced Larmor precession frequencies of the spin(s).

There is a principal difference between the route to chaos by cascades of period-doubling bifurcations and the route by irregular periods. The cascades of period-doubling bifurcations occur in the periodic regime. They indicate the proximity of a chaotic regime and, using Feigenbaum's universality,[16] they predict the critical parameter values for the transition to the chaotic regime.

In contrast, we have characterized the route to chaos by irregular periods according to the behavior in the chaotic regime close to the transition from regular to irregular behavior. It is too early to infer that this route fits into the quasiperiodic to turbulent transition described by Ruelle and Takens,[17] although the limit cycles observed in the periodic regime are examples of quasiperiodicity. The point is that the nonlinearity of the spin motion implies a self-detuning of the Larmor frequency when the precession angle is changed. This fact seems also to be important for some kind of intermittency[18] found in the multispin system. It is beyond the scope of this paper to analyze this type of chaos in more detail. The aim was to find simple models close to the experimental arrangements of parallel-pumping experiments and to simulate qualitatively the measured regular and irregular "relaxation oscillations."

## ACKNOWLEDGMENTS

The authors would like to thank E. Brun, W. Floeder, L. A. Lugiato, P. F. Meier, B. D. Patterson, and D. F. Walls for their valuable help and encouraging interest, and the Swiss National Science Foundation for the financial support.

[1]For reviews see, e.g., J.-P. Eckmann, Rev. Mod. Phys. **53**, 643 (1981); *Order in Chaos,* Proceedings of the Conference at Los Alamos, 1982, edited by D. Campbell and H. Rose [Physica **7D** (1983)]; *Dynamical Systems and Chaos,* Proceedings of the International Conferences, Sitges, Barcelona, Spain, 1982, Vol. 179 of *Lecture Notes in Physics,* edited by L. Garrido (Springer, Berlin, 1983).

[2]H. Yamazaki, J. Phys. Soc. Jpn. **53**, 1155 (1984).

[3]K. Nakamura, S. Ohta, and K. Kawasaki, J. Phys. C **15**, L143 (1982).

[4]G. Gibson and C. Jeffries, Phys. Rev. A **29**, 811 (1984).

[5]T. S. Hartwick, E. R. Peressini, and M. T. Weiss, J. Appl. Phys. **32**, 223S (1961).

[6]D. R. Barberis, F. Waldner, and H. Yamazaki, *Proceedings of the XXII Congress AMPERE on Magnetic Resonance and Related Phenomena, Zürich,* edited by K. A. Müller, R. Kind, and J. Roos (Zürich Ampère Committee, University of Zürich, Zürich, 1984), pp. 149 and 150.

[7]V. V. Zautkin and S. S. Starobinets, Fiz. Tverd. Tela (Leningrad) **16**, 678 (1974) [Sov. Phys.—Solid State **16**, 446 (1974)].

[8]V. I. Ozhogin and A. Yu. Yakubovskii, Zh. Eksp. Teor. Fiz. **67**, 287 (1974) [Sov. Phys.—JETP **40**, 144 (1975)].

[9]V. E. Zakharov, V. S. L'vov, and S. S. Starobinets, Usp. Fiz. Nauk **114**, 609 (1974) [Sov. Phys.—Usp. **17**, 896 (1975)].

[10]V. L. Grankin, V. S. L'vov, V. I. Motorin, and S. L. Musher, Zh. Eksp. Teor. Fiz. **81**, 757 (1981) [Sov. Phys—JETP **54**, 405 (1981)].

[11]L. A. Lugiato, L. M. Narducci, D. K. Bandy, and C. A. Pennise, Opt. Commun. **46**, 64 (1983).

[12]F. Keffer, *Encyclopedia of Physics,* edited by S. Flugge, and H. P. J. de Wijn (Springer, Berlin, 1966), Vol. XVIII/2, pp. 1—273, and references therein.

[13]E. Brun, B. Derighetti, R. Holzner, and M. Ravani, Acta Phys. Austriaca (to be published); E. Brun, B. Derighetti, D. Meier, R. Holzner, and M. Ravani, in *Instabilities in Optical Active Media,* edited by N. B. Abraham, L. A. Lugiato, and L. M. Narducci, Vol. 2B of J. Opt. Soc. America-JOSAB (American Institute of Physics, New York, 1985).

[14]F. Waldner, J. Magn. Magn. Mater. **31—34**, 1015 (1983).

[15]A. R. Bishop, K. Fesser, P. S. Lomdahl, W. C. Kerr, M. B. Williams, and S. E. Trullinger, Phys. Rev. Lett. **50**, 1095 (1983).

[16]M. J. Feigenbaum, J. Stat. Phys. **19**, 25 (1978).

[17]D. Ruelle and F. Takens, Commun. Math. Phys. **20**, 167 (1971).

[18]P. Manneville and Y. Pommeau, Phys. Lett. **75A**, 1 (1979).